Published in final edited form as:
Ann Biomed Eng. 2011 May ; 39(5): 1570–1581. doi:10.1007/s10439-010-0242-9.

NET CHANGE IN PERIOSTEAL STRAIN DURING STANCE SHIFT LOADING AFTER SURGERY CORRELATES TO RAPID DE NOVO BONE GENERATION IN CRITICAL SIZED DEFECTS

Sarah H McBride[1], **Scott Dolejs**[1], **Stefano Brianza**[2], **Ulf Knothe**[3], and **Melissa L Knothe Tate**[1]

[1]Case Western Reserve University, Cleveland, OH [2]AO Foundation, Davos, Switzerland
[3]Cleveland Clinic Foundation, Cleveland, OH, USA

Abstract

In an ovine femur model, proliferative woven bone fills critical sized defects enveloped by periosteum within two weeks of treatment with the one stage bone transport surgery. We hypothesize that mechanical loading modulates this process. Using high-definition optical strain measurements we determined prevailing periosteal strains for normal and surgically treated ovine femora subjected *ex vivo* to compressive loads simulating *in vivo* stance shifting (n=3 per group, normal versus treated). We determined spatial distribution of calcein green, a label for bone apposition in first the two weeks after surgery, in 15°, 30°, and 45° sectors of histological cross sections through the middle of the defect zone (n=6 bones, 3–4 sections/bone). Finally, we correlated early bone formation to either the maximal periosteal strain or the net change in maximal periosteal strain. We found that treatment with the one stage bone transport surgery profoundly changes the mechanical environment of cells within the periosteum during stance shift loading. The pattern of early bone formation is repeatable within and between animals and relates significantly to the actual strain magnitude prevailing in the periosteum during stance shift loading. Interestingly, early bone apposition after the surgery correlates more to the maximal net change in strain (above *circa* 2000–3000 με, in tension or compression) rather than strain magnitude *per se*, providing further evidence that changes in cell shape may drive mechanoadaptation by progenitor cells. These important insights regarding mechanobiologic factors that enhance rapid bone generation in critical sized defects can be translated to the tissue and organ scale, providing a basis for the development of best practices for clinical implementation and the definition of movement protocols to enhance the regenerative effect.

Keywords

periosteum; mechanical loading; mechanobiology; progenitor cells; mechanics; endogenous tissue engineering

CORRESPONDING AUTHOR: Dr. Melissa Knothe Tate, 10900 Euclid Ave, Wickenden 512, Cleveland, OH, USA 44106, Phone: 216-368-5884, Fax: 216-368-4969, KnotheTate@case.edu.

CONFLICTS OF INTEREST:
All authors have no conflicts of interest.

Introduction

There is a significant correlation between mechanical loading and the amount and density of early (within two weeks of surgery) bone generated in critical sized segmental bone defects that are enveloped *in situ* by periosteum (one stage bone transport procedure, Fig. 1).[21] Namely, along the long bone axis least able to resist bending loads (minor centroidal axis, CA), bone laid down in the first two weeks after surgery exhibits more mineralization albeit less total area compared to bone along the axis most able to resist bending loads (major CA). Similarly, areas of the cross section along the minor CA show a higher degree albeit less total area of vascular perfusion compared to bone along the major CA.[21] Furthermore, spatial maps reveal a radial distribution of early bone generation, highest near the periosteum and decreasing toward the surface of the intramedullary nail, which fills the medullary cavity; these observations are indicative of periosteum-derived *de novo* bone formation in the defect.[21] Interestingly, recent studies also show that osteochondral progenitor cells, such as those residing in the periosteum, exhibit a greater than thousand fold sensitivity to mechanical signals than terminally differentiated cells such as osteoblasts, when subjected *in vitro* to controlled loading regimes[24,38] Taken together, these studies provided the impetus for our current work, i.e. to elucidate prevailing mechanical strains in the periosteum during stance loading, in normal femora and immediately after treatment with the one stage bone transport procedure. Ultimately, we aimed to correlate quantitative changes in mechanical loads experienced by the periosteum to periosteum-derived *de novo* bone formation observed within the defect zone in the first two weeks after the one stage bone transport procedure.

The periosteum is a bilayered membrane that envelops bones.[2, 3, 21] The outer layer is comprised of mostly collagens and elastin. This layer is hypothesized to control bone shape/length during growth,[41] to contribute to bone toughness, and to stabilize bones during failure by limiting bone end displacements during fracture.[45] The periosteum's innermost layer, closest to the bone, is comprised mostly of cells. The progenitor cells within the inner layer are responsible for continual, baseline periosteal bone apposition[37] as well as bone and cartilage regeneration during fracture repair.[7, 28, 46] Furthermore, it is hypothesized that the progenitor cells within the inner periosteal layer are responsible for the rapid large-scale bone generation observed in the first two weeks after application of the one stage bone transport procedure[18, 19] as well as after other surgical techniques such as periosteal distraction[15, 34, 36, 44] and periosteal tenting.[44]

As mentioned previously, osteochondral progenitor cells and mesenchymal stem cells (MSCs), such as those residing in the periosteum, are very sensitive to their mechanical environment.[18, 24, 32] Mechanical factors, such as the area available to spread,[22] stiffness of the underlying matrix,[10, 23] matrix strain, fluidic shear stress,[24] fluidic pressure, and temporal characteristics of loading (e.g. static versus oscillatory stimulation) can affect stem cell differentiation. In fact, previous *in vitro* studies indicate that osteoblasts differentiated from periosteal progenitor cells are more mechanically sensitive then osteoblasts differentiated bone marrow derived stem cells.[13] Typically, tension (stretching) or shear stress is associated with differentiation of MSCs into osteogenic cells.[4, 18] Compression is associated with differentiation of MSCs into chondrogenic cells.[18] From the cell's perspective, the mechanical environment of the periosteum is likely defined by prevailing deviatoric, shape changing, stresses[4] due to the sheath like geometry and highly anisotropic material properties of periosteal tissue. With the typical differentiation response of MSCs to mechanical loading in mind, it follows that periosteal progenitor cells would react to the changes in mechanical loading applied to the periosteum on a tissue level. Hence in the current study, we hypothesize that areas of periosteum subjected to deviatoric strain during

compressive loading correlate to areas of rapid initial bone generation observed in conjunction with the one stage bone transport procedure.

To test this hypothesis, we developed methods to measure strain optically in the periosteal sleeve during compressive loading cycles that mimic the physiologic condition when sheep shift stance during the first two weeks after the one stage bone transport procedure. Strains measured *ex vivo* in periosteum surrounding the defect zone during stance shift loading were compared between those measured *ex vivo* after treatment with the one stage bone procedure and the normal, contralateral periosteum. We then determined whether strain measurements correlated to the amount of bone generated during the first two weeks after surgery (a histomorphometric outcome measure carried out after *in vivo* studies). A correlation indicates a relationship between mechanical stimuli and the early bone apposition observed in the first two weeks after the treatment.

Materials & Methods

This study was accomplished in three steps. First, we used optical methods to measure *ex vivo* changes in prevailing strain patterns of the periosteum during stance shift loading that could be attributed to treatment with the one-stage bone transport surgical technique,[19, 20] (see Fig. 1 for full details of the surgical procedure). Second, we analyzed histological samples from the previous *in vivo* study of the one stage bone transport procedure to determine the distribution of bone generated during the first two weeks of healing. Third, we determined whether areas of altered strain distribution, identified through optical strain mapping, correlated to the histomorphometric measures of bone apposition during early time periods after the surgical procedure. A significant correlation between areas of altered strain and areas of initial bone apposition is indicative of a relationship between the mechanical environment of the periosteum and early bone apposition after treatment.

Ex Vivo Optical Strain Mapping of Normal and Post-surgical Femora

Immediately after euthanasia, whole ovine femora were explanted and then either left intact (normal, control, n = 3) or subjected to the one-stage bone transport surgical technique (post-surgery, experimental, n = 3) by the same surgeon who conceived of the one stage bone transport technique.[19, 20] To prepare for *ex vivo* loading, the femoral condyles were first embedded in polymethalmethacrylate (PMMA) to ensure a secure interface with the bottom grip of the mechanical tester. Then a contrasting paint was speckled onto the periosteum-enveloped femoral diaphysis to observe strain patterns under load. Next, the femur was tested using a servo-hydraulic material testing machine (MTS Bionix 858, MTS Systems Co., Eden Prairie, MN) with a six-degree of freedom load cell (4kN, 250 Nm, HUPPERT 6, HUPPERT GmbH, Herrenberg, Germany) and custom made grips that apply a compressive load in physiological directions (Figure 2A). The distal grips constrain the femoral condyles up to just proximal of the patellar surface. The proximal grip interfaces with the femoral head but does not constrain its rotational movement. A compressive load was applied in stepwise fashion (each load step was hold for 10 seconds) to a load approximating one times body weight (~700N), to mimic stance shift loading during the two weeks after surgery, when the sheep are protected by a torso sling that allows weight bearing but prevents impact loading and direct pressure to the skin closed over the surgical site.[42] During the two weeks after surgery, the sheep shift their weight during waking hours and relax into the sling during sleep.

The PMMA embedded condyles settled into the testing grip during the first loading cycle, which was not included in our analysis. The loading cycle was repeated 15–17 times for each femur. For all tests the following parameters were recorded at a sampling frequency of

64 Hz: axial displacement of the actuator (mm) acquired by the MTS machine, axial load (N) acquired by the load cell.

To monitor strain fields in the periosteum during *ex vivo* loading, the spatiotemporal pattern of the previously applied paint speckles (on surface of the proximal femur) was recorded using a high definition video camera (XDCAM HD, Sony Co., New York, NY), from the anterior, lateral and posterior vantage points (Figure 2B). After recording the compressive test data, the video footage was separated into 1 frame/sec still images using video editing software (Final Cut Pro 7, Apple Co., Cupertino, CA). The still images were analyzed using our custom designed MatLab program (The MathWorks Co., Natick, MA) that utilizes the digital image correlation function (cpcorr) to track movement of the contrasting dots applied before compressive testing.

To summarize, the optical strain mapping technique involved using a customized MatLab program to define the grid points to be used with MatLab's built in “cpcorr function” and to calculate strains from the displacement measurements. Basically, the cpcorr function requires the user to define a set of “grid points” that are tracked from frame to frame. A key part of the tracking algorithm is detection of contrast within the immediate area of the grid point. For this reason we wanted to only track points at the edge of the speckles and not the interior of any speckle. So, starting with the first image (base image) the user defines the left and right sides of the plane of focus. The computer then selects all pixels that are speckled white within the user defined boundaries (i.e. the entire areas that are speckled). The user is then given the option to change the threshold that is defined as “white” in case some speckles are being picked up as grey and are thus not being marked and tracked. After satisfactorily marking all white pixels in the plane of focus, the computer automatically eliminates pixels from the interior of speckles by removing any points that are surrounded on all eight neighboring sides by other white pixels. This effectively marks all the pixels on the border of each speckle. Then, to reduce computational time, the marked border pixels are "thinned" so that only one pixel in a 11×11 pixel area is tracked. Then, the user has the option to remove areas of inappropriately marked pixels (e.g. in areas extraneous to the periosteal mechanics research question at hand, such as those tracking reflections off a screw head) as well as to provide additional individual pixels (in case areas of interest were automatically removed in the previous step). The x and y co-ordinates of these marked pixels are then obtained and given to the cpcorr function along with the base image and the next frame. The cpcorr function returns the new co-ordinates of the same landmark points in the next frame. The process is repeated until the same landmarks are tracked through all available frames. Then, using these displacements, the strains are calculated.

The average strain between a point and any other tracked points within a 200–400 pixel range was calculated based on pixel displacements. Two types of strain were measured during multiple stance loading cycles, including (i) the actual strain on the outer surface of the periosteum, immediately after surgical treatment, and (ii) the difference between the actual strain (immediately after treatment) and equivalent strains in the identical areas of periosteum of untreated femora. The net strain calculated in (ii), reflects the change in the mechanical strain environment of the periosteum during stance loading that is attributable to treatment with the one stage bone transport surgery. A mean and standard deviation was first calculated for each femur and then for each group of femora, based on the individual means.

Analysis of Initial Bone Distribution

Bone distribution was calculated in samples from a previous *in vivo* study of the one stage bone-transport surgical technique.[21] In these studies, calcein green flourochrome was administered intravenously at 2–3 weeks after surgery. The flourochrome chelates to mineralizing tissue between the time of injection and clearance from the urine.[21, 30, 31] The

sheep were euthanized 16 weeks after surgery and the entire femur, including soft tissue, was removed and fixed in a PMMA without prior decalcification. The center of the defect zone was then cut into approximately 250 μm cross sections using a diamond wire saw (Well Diamond Wire Saws, Norcross, GA), polished to approximately 100 μm, and coverslipped for imaging under the microscope. Three to four cross sections, cut through the middle of the defect zone, were analyzed histologically (n=6 femora).[21]

For the current study, the previously prepared samples were imaged with UV light (Leica Filter System A, excitation filter broad pass 340–380 nm, dichroic mirror 400 nm, barrier filter low pass 430 nm) as well as blue light, on an epifluorescence inverted microscope with motorized stage control and full color camera, at 5x magnification (Leica DMIRE2 automated inverted microscope, Leica, Germany). The UV light excites all autofluorescent collagen-containing areas of the cross-section (muscle, bone, fibrous tissue) (Figure 3A) while the blue light excites only the chelating agent administered at 2–3 weeks of healing (Figure 3C).

The anatomical axes were defined by locating the center of the intramedullary nail (visible in the UV excitation image). The axis directions were determined by creating a ray between the nail center and the mid-posterior aspect, defined by the anatomical reference point where the trochanteric crest intersects with the insertion of the *quadratus femoris*. The posterior axis was defined by the ray and all other axes were determined relative to the posterior axis (Figure 3B). Now, using the anatomical axes, the percent of total initial bone generation, as measured by number of pixels exhibiting green fluorescence, was quantified using MatLab for 15°, 30°, and 45° sectors around the cross section's circumference. The 15°, 30°, and 45° sectors were chosen to resolve the cross sectional area spatially and observe general trends without amplifying an individual sample's trends. One sample was excluded from the study due to insufficient calcein green emission at the image resolution of interest to this study (no analysis possible).

Outcome measure data was fit to a general linear model (1) created in MatLab to determine i) if the early bone formation differed from bone to bone or was similar in all bone samples, ii) if the early bone formation differed significantly from section to section (serial sections) within a bone, and iii) if the early bone formation differed significantly from sector to sector. Significance was defined by $p < 0.05$ for the linear coefficient of any predictor.

$$PercentEarlyBone=\beta_0+\beta_1 Bone+\beta_2 Section+\beta_3 Sector \quad (1)$$

Correlation of Strain and Initial Bone Formation

After analyzing the mechanical environment (actual and net change in strain due to operative treatment) in the periosteum surrounding the defect area during the first two weeks of healing of the one-stage bone transport system, as well as the distribution of early bone apposition after the treatment, the two measures were compared to determine correlation. While the strains of the periosteum surrounding entire defect area were calculated as part of this study, only the strains of the periosteum surrounding the middle of the defect cross section (or corresponding area in the normal femur) were utilized to maximize comparison with histological samples. One of three general linear models were used to determine the relationship between strain and bone generation. The three models were chosen after examining the trends observed in the pilot data. The first model was a linear model (2), the second was a quadratic model (3), and the third was an absolute value model (4). Significance was defined by $p < 0.05$ for the linear coefficient of any predictor.

$$PercentEarlyBone=\beta_0+\beta_1 Strain \quad (2)$$

$$PercentEarlyBone=\beta_0+\beta_1 Strain+\beta_2 Strain^2 \quad (3)$$

$$PercentEarlyBone=\beta_0+\beta_1 |Strain| \quad (4)$$

Statistics

All graphs (Figure 4 & 5) report average value with 95% confidence intervals except for the box plot figures used for correlation (Figure 6). All statistics were carried out using the general linear model function of MatLab using the respective equations listed above. In all cases, a $p < 0.05$ indicates significance of that predictor.

Results

Ex Vivo Optical Strain Mapping of Normal Femora and Femora after Surgical Treatment

Periosteal strains were measured optically during *ex vivo* loading to mimic stance shift in non-operated and operated femora (Figures 2 & 4). During stance loading of the non-operated femur, tension dominates in the anterior aspect and compression dominates in the posterior aspect. After treatment, the periosteal strain environment is altered completely, with compression prevailing in the anterior aspect and tension dominating in the posterior aspect (Figure 4 & Table 1).

Along the middle of the defect cross sections where histological outcome measures were determined, operative treatment results in a profound change in the mechanical environment of the periosteum during exposure to stance loading compared to that in the non-operated femur. In the non-operated femur, the periosteum along the anterior aspect of the comparable transverse midline experiences tensile strains, starting with 0 microstrain (με, 0%) at initiation of the loading cycle, reaching a maximum of *circa* 3000 to 3100 με in tension (0.3% lengthening) at maximal loading, and returning to 0 με at the end of the loading cycle. Immediately following operative treatment, periosteum in the same area reaches a maximum of *circa* −2900 to −3500 με in compression (0.3% shortening) at maximal loading. Hence, as a consequence of surgical treatment, the maximum net change in the anterior periosteum's mechanical environment can be as much as −6000 με (0.6% shortening). Periosteum along the posterior aspect of the midline in a normal femur can experience compressive strains of 0 με at initiation and end of loading, reaching a maximum of *circa* −2950 to −3050 με (0.3% shortening) at maximal loading. Periosteum located in the same area of operated femora experience tensile strains of 0 με at initiation of loading and end of loading, reaching a maximum of *circa* 650 to 1000 με (0.065–0.1% lengthening) at maximal loading. Hence, the net maximal change in the posterior periosteal environment comprises 3900 με (0.39% lengthening) as a consequence of operative treatment. Periosteum along the lateral aspect of the midline in a non-operated femur experiences compressive or tensile strains of 0 με at initiation and end of loading, reaching a maximum of −800 to 800 με (0.08% lengthening or shortening) at maximum loading. Immediately following treatment, the same periosteum can experience compressive or tensile strains of 0 με at initiation of loading and end of loading, reaching −1800 to 100 με (0.18% shortening to 0.01% lengthening) at maximum loading. Hence, the lateral periosteum experiences a maximal net change in its mechanical environment of −2400 με (0.24% shortening) due to operative treatment. Thus, periosteum in lateral areas of the defect cross section are

subjected to a change in mechanical environment roughly half way between those experienced along the anterior and posterior aspects, respectively.

Analysis of Initial Bone Distribution

The distribution of early bone generation was determined using three different sector sizes (15°, 30°, and 45°) (Figure 3 & 5). For all sector sizes, significant differences are attributable to the sector under study (p-values for sector is the only significant predictor) but not to the bone or section examined (no significant difference in early bone formation between, i.e. bone to bone, or within, i.e. section to section, bone samples). In general, the most early bone generation occurs just medial of anterior, followed by early bone apposition occurring in the posterior aspect. Early bone apposition in the medial area, interposed between the anterior and posterior aspects, is evenly distributed and comprises roughly half the early bone apposition observed in the anterior aspect. In contrast, bone apposition in the lateral area, interposed between the anterior and posterior aspects, gradually declines, going from the anterior to just before the posterior sector, where little early bone apposition is evident.

Correlation of Strain and Initial Bone Formation

First we determined if there is a correlation between the amount of early bone apposition in a given sector and the average maximum strain (actual and net change due to operative treatment) (Figure 6, Tables 2 & 3). Regardless of sector size, the actual periosteal strain (range measured: −3600 to 1000 με) relates significantly, and in a negative linear relationship, to early bone apposition (Table 2). Furthermore, the net change in periosteal strain due to operative treatment exhibits either a quadratic or an absolute value relationship to early bone apposition, regardless of sector size examined ($p < 0.05$) (Table 3).

Discussion

Treatment with the one stage bone transport surgery profoundly changes the mechanical environment of cells within the periosteum. Based on strains measured in the periosteum during exposure to stance shift loading *ex vivo*, early bone apposition after the surgery correlates more to the maximal net change in strain during stance loading rather than strain magnitude itself. If the observed rapid proliferative woven bone generation within the defect were the result of periosteal lifting or some other aspect of the one stage bone transport procedure *per se*, we would have expected to observe no correlation between changes in loading patterns and amount of bone formation in different zones of the defect. Interestingly, we observed a negative linear relationship between measured periosteal strain magnitude and early bone apposition, indicating that tensile loading is not prerequisite for early bone apposition by the periosteum. In fact, the amount of bone formation in the first weeks after the one stage bone transport surgery best fits a quadratic or absolute value function to the net change in periosteal strain magnitude experienced during stance loading. Taking these insights into consideration, a net absolute (tensile or compressive) change in strain exceeding *circa* 2000 – 3000 με enhances initial bone formation by periosteal cells. Our current working hypothesis is the one stage bone transport surgery places osteochondral progrenitor cells in a new mechanical and biochemical environment, that triggers rapid adaption through proliferation, egression from the periosteum into the defect and/or secretion of extracellular matrix proteins that ultimately make up the osteoid (which mineralizes to bone and is chelated by the fluorchrome administered during this time period). Any one or a combination of events including cell proliferation, egression, and or matrix secretion could result in more bone formation within the defect. In light of previous studies showing a radial distribution of early intramembranous bone formation from the periosteum to the surface of the intramedullary nail[21] and increased regenerative capacity of

the periosteum with mechanical loading,[29, 43] it is likely that mechanically modulated transport of cells and biochemical factors also plays a role in the remarkable regenerative capacity of the periosteum.

Although a rich body of literature describes the role of mechanical loading in healing of fractures, the role of mechanical loading in the osteogenic capacity of the periosteum has been less well understood. In early canine studies, Puckett *et al.* discovered a 62% decrease in the capacity of grafted periosteum to regenerate diaphyseal defects when transferred to the non-weight bearing fibula compared to the tibia.[29] Puckett *et al.* concluded that mechanical stress transfer through weight bearing is a necessary stimulus for the periosteum to form new bone. This is further supported by data showing that, when grafted to a defect in a weight-bearing site, calvarial periosteum forms bone with five times the mechanical strength of that resulting from *in situ* grafting in the calvarium.[43] Our previous study also shows a statistically significant correlation between de novo bone formation in segmental defects, mechanical loading, and proximity to the periosteum.[21] In our current studies, the change in mechanical environment of the periosteum that is attributable to treatment with the one stage bone transport relates to the combined effects of periosteal release and subsequent surgical reattachment to the bone at the distal edge of the defect zone as well as to changing (straightening) of the overall femoral geometry by introduction of the straight intramedullary nail. The experimentally measured strain fields of the current study confirm the conceptual shift in strain field expected for an elastic sheet sheathing a curved beam. If a prestressed elastic sheet like the periosteum is released from a curved beam, the area corresponding to the convex aspect of the beam relaxes and the area corresponding to the concave aspect stretches relative to its original state. Thereafter, if the beam is straightened and the elastic sheet then fixed to the new geometry, the boundary conditions are changed; the areas previously in tension are now fixed in a more relaxed state and the areas previously in compression (in the "crook of the elbow") are now fixed in a more tensed state. Hence, changing the baseline state of the periosteal tissue profoundly changes the mechanical milieu of the cells immediately after the surgery as well as during the first two weeks after surgery when the femur is subjected to stance shift loading. In changing the mechanical milieu, the surgery must also affect transport of cells and anabolic factors from the periosteum to the surface of the intramedullary nail.

The observation of significant proliferative woven bone formation in defects surrounded by periosteum *in situ*[17, 19] and generation of bone through static periosteal elevation (termed periosteal tenting)[44] or dynamic elevation (termed periosteal distraction)[15, 34, 36, 44] provides ample evidence for the mechanosensitivity and bone building capacity of periosteum derived cells. From the cell's perspective, the local strain field and how it changes from the baseline condition, is what drives adaptation, either directly through shape induced fate decisions[18] or indirectly through augmentation of molecular and cellular transport via fluid flow[17]. Hence, from the perspective of a given cell within a specific area of the periosteum, it is unlikely that the direction of loading is key; rather the imposed change in "shape" (dictating the boundary conditions) of the cell's immediate surroundings is the likely means by which the cell senses and adapts to the change in mechanical environment [as reviewed in Knothe Tate et al. 2008[17], and reported on in a model embryonic derived mesenchymal stem cell line by Song et al. 2010[38], Chang et al. 2010[6], Zimmerman et al. 2010[47]]. Although three-dimensional measures of the cell's strain enviroment, using the cell as an absolute reference point, would be ideal for full spatiotemporal characterization, such measures are currently not feasible. Interestingly, given our recent data showing anisotropy in the elastic modulus of periosteum (axial versus circumferential directions), we know with certainty that a given periosteal strain (compressive or tensile) will result in a change in shape of a cell within the periosteum[18] as well as the development of pressure gradients within the defect zone

spanning between the inner surface of the periosteum and the outer surface of the intramedullary nail in the first two weeks after the one stage bone transport surgery[26].

In addition, previous studies have proven the release of osteogenic factors by isolated explanted periosteal cells exposed to tensile substrate strain in the absence of fluidic shear strain.[13],[14] Furthermore, a number of published studies describe the migration, proliferation, and biochemical differentiation of isolated periosteal cells.[5, 9, 11, 27, 33, 39] Within days in culture, periosteal cells egress from periosteal explants and proliferate.[5, 14] These periosteum derived cells show superior osteogenic capacity when compared to bone marrow derived stem cells.[11, 27, 33] In fact, a significant fraction of periosteum derived cells will differentiate into an osteogenic lineage even when cultured in non-supplemented culture media[27] or adipogenic media.[5]

The correlation between the mechanical environment and early bone formation reported in this study does not preclude the importance of biochemical factors, and it is likely that biophysical and biochemical factors act synergistically to modulate new bone formation. In one periosteal tenting study, bone formation was only noted if calcium was included in the alginate gel used to raise the periosteum above the surface of the cortical bone.[40] Interestingly, in our previous *in vivo* one stage bone transport study, the retention of small cortical bone chips on the inner surface of the periosteum resulted in superior regenerate bone density.[19, 20] Furthermore, recent studies from our group demonstrate the capacity of isolated periosteal cells seeded on collagen sponges within a flow directing implant to generate bone in critical sized long bone defects.[16] In the same study, superior bone generation is achieved when strips of periosteum are resected and placed within the flow directing implant, suggesting that factors within the periosteal tissue itself contribute to early bone formation.[16] Furthermore, if oscillatory strain results in convective flow, the flow may augment release of biochemical factors as well as osteochondral progenitor cells from the periosteum and their radial distribution into the center of the defect. Biochemical factors can act synergistically with mechanical signals such as strain and shear stress to promote early bone formation as seen in mesenchymal stem cells.[8, 12] Although we know of no published studies of periosteal cells exposed to shear stress to date, we expect them to upregulate genes similar to embryonic cells derived from the mesoderm during mesenchymal condensation, the first step of skeletogenesis.[18]

Every experimental model has limitations in its ability to mimic dynamic physiological conditions. Since it is not currently possible to assess the mechanical environment of the periosteum over time in a living animal, we used an *ex vivo* model to measure strains optically during mechanical loading designed to mimic shift in stance, which is the primary mode of loading in the first two weeks after surgical treatment with the one stage bone transport procedure. Furthermore, in order to observe strains using optical speckling of the periosteum, we had to remove soft tissues surrounding the periosteum including the musculature. Lastly, in this study we report the correlation between maximal oscillatory strain and early bone formation. The measured oscillatory strain does not account for the prestrain imposed on the periosteum by stretching it and suturing it to the denuded bone segment (estimated at 10% lengthening). This prestrain may relax over time or may act to amplify effects of the oscillatory strain imposed on the periosteum during stance. In any case, by measuring the difference in strain state of the periosteum in operated and non-operated femora, we account for the difference in mechanical stress state attributable to treatment, which includes the prestrain applied through suturing of the periosteum to envelop the defect.

In combination with our recently published study demonstrating the radial distribution of the calcein green label, from the periosteal sheath, toward the intramedullary nail, it appears that

the profound change in mechanical and biochemical state at the time of surgery exerts a trigger effect that then results in subsequent egression of cells and then direct intramembranous bone formation. Due to the radial distribution of the calcein green label and its relation to mechanical loading state, as shown in a recently published study from our group,[21] the formation of intramembranous bone is related both to periosteal as well as mechanical factors. The current study elucidates, on the one hand, what those mechanical factors are at the time of surgery, as well as how they relate to the formation of bone in the two weeks after surgery. Follow on studies are underway to better understand the cellular mechanisms of rapid proliferative bone formation via the periosteum. Clinical studies will be important to best harness the healing and tissue generating capacity of the periosteum for different cell populations (e.g. autologous chondrocyte versus periosteum-derived cells implantation for cartilage versus bone defect repair). Ultimately, the current study may help to establish guidelines for post surgical protocols (e.g. >2000–3000 oscillatory με stimulation) and points to physical therapy as an adjuvant to augment biophysiologic outcomes.

Acknowledgments

These studies were supported through a grant from the AO Foundation (F-07-99K). Sara McBride was supported through an NIH Training grant (NIH/NIAMS T32 AR007505). In addition, we would like to acknowledge Boyko Gueorguiev-Rüegg, Chris Roberts and Dr. Steven Sidik for their respective assistance with mechanical loading, image analysis and statistics.

References

1. Alexander D, Schäfer F, Munz A, Friedrich B, Klein C, Hoffmann J, Buhring H, Reinhert S. LNGFR induction during osteogenesis of human jaw periosteum-derived cells. Cell. Physiol. Biochem. 2009; 24:283–290. [PubMed: 19710543]
2. Allen MR, Burr DB. Human femoral neck has less cellular periosteum, and more mineralized periosteum, than femoral diaphyseal bone. Bone. 2005; 36:311–316. [PubMed: 15780957]
3. Allen MR, Hock JM, Burr DB. Periosteum: biology, regulation, and response to osteoporosis therapies. Bone. 2004; 35:1003–1012. [PubMed: 15542024]
4. Anderson EJ, Knothe Tate ML. Design of tissue engineering scaffolds as delivery devices for mechanical and mechanically modulated signals. Tissue Eng. 2007; 13:2525–2538. [PubMed: 17822359]
5. Arnsdorf EJ, Jones LM, Carter DR, Jacobs CR. The periosteum as a cellular source for functional tissue engineering. Tissue Eng. A. 2009; 15:2637–2642.
6. Chang H, Knothe Tate ML. Anisotropic Adaptation of C3H/10T1/2 Model Stem Cell Line to Changing Mechanical Environments. Ann. Biomed. Eng. 2010 In Submission.
7. Colnot C. Skeletal cell fate decisions within periosteum and bone marrow during bone regeneration. J. Bone Miner. Res. 2009; 24:274–282. [PubMed: 18847330]
8. Datta N, Pham QP, Sharma U, Sikavitsas VI, Jansen JA, Mikos AG. In vitro generated extracellular matrix and fluid shear stress synergistically enhance 3D osteoblastic differentiation. Proc. Natl. Acad. Sci. U. S. A. 2006; 103:2488–2493. [PubMed: 16477044]
9. De Bari C, Dell'Accio F, Karystinou A, Guillot PV, Fisk NM, Jones EA, McGonagle D, Khan IM, Archer CW, Mitsiadis TA, Donaldson AN, Luyten FP, C Pitzalis. A biomarker-based mathematical model to predict bone-forming potency of human synovial and periosteal mesenchymal stem cells. Arthritis Rheum. 2008; 58:240–250. [PubMed: 18163504]
10. Engler AJ, Sen S, Sweeney HL, Discher DE. Extracellular matrix elasticity directs stem cell lineage specification. Cell. 2006; 126:645–647. [PubMed: 16923382]
11. Hayashi O, Katsube Y, Hirose M, Ohgushi H, Ito H. Comparison of osteogenic ability of rat mesenchymal stem cells from bone marrow, periosteum, and adipose tissue. Calcif. Tissue Int. 2008; 82:238–247. [PubMed: 18305886]

12. Holtorf HL, Jansen JA, Mikos AG. Flow perfusion culture induces the osteoblastic differentiation of marrow stroma cell-scaffold constructs in the absence of dexamethasone. J. Biomed. Mater. Res., Part A. 2005; 72:326–234.
13. Jones DB, Nolte H, Scholübbers JG, Turner E, Veltel D. Biochemical signal transduction of mechanical strain in osteoblast-like cells. Biomaterials. 1991; 12:101–110. [PubMed: 1652292]
14. Kanno T, Takahashi T, Ariyoshi W, Tsujisawa T, Haga M, Nishihara T. Tensile mechanical strain up-regulates Runx2 and osteogenic factor expression in human periosteal cells: implications for distraction osteogenesis. J. Oral Maxillo. Surg. 2005; 63:499–504.
15. Kessler P, Bumiller L, Schlegel A, Birkholz T, Neukam FW, Wiltfang J. Dynamic periosteal elevation. Brit. J. Oral Maxillo. Surg. 2007; 45:284–287.
16. Knothe Tate ML, Chang H, Knothe U. Role of periosteal factors in long bone defect healing. Proc. 56th Ann. Ortho. Res. Soc. 2010:0384.
17. Knothe Tate M, Falls TD, Mishra S, Atit R. Engineering an ecosystem: taking cues from nature's paradigm to build tissue in the lab and the body. Fields Inst. Com. 2010; 57 Available Online.
18. Knothe Tate ML, Falls TD, McBride SH, Atit R, Knothe UR. Mechanical modulation of osteochondroprogenitor cell fate. Int. J. Biochem. Cell Bio. 2008; 40:2720–2738. [PubMed: 18620888]
19. Knothe Tate ML, Ritzman TF, Schneider E, Knothe UR. Testing of a new one-stage bone-transport surgical procedure exploiting the periosteum for the repair of long-bone defects. J. Bone Joint Surg. Am. 2007; 89:307–316. [PubMed: 17272445]
20. Knothe UR, Springfield DS. A novel surgical procedure for bridging of massive bone defects. World J. Surg. Oncol. 2005; 3:7. [PubMed: 15691380]
21. Knothe UR, Dolejs RM, Miller ML. Knothe Tate, Effects of mechanical loading patterns, bone graft, and proximity to periosteum on bone defect healing. J Biomech. 2010; 43:2728–2737. [PubMed: 20673900]
22. McBeath R, Pirone DM, Nelson CM, Bhadriraju K, Chen CS. Cell shape, cytoskeletal tension, and RhoA regulate stem cell lineage commitment. Dev. Cell. 2004; 6:483–495. [PubMed: 15068789]
23. McBride SH, Knothe Tate ML. Modulation of stem cell shape and fate A: the role of density and seeding protocol on nucleus shape and gene expression. Tissue Eng. A. 2008; 14:1561–1572.
24. McBride SH, Falls T, Knothe Tate ML. Modulation of stem cell shape and fate B: mechanical modulation of cell shape and gene expression. Tissue Eng. A. 2008; 14:1573–1580.
25. McBride SH, Dolejs S, Knothe U, Knothe Tate ML. Major and Minor Centroidal Axes Serve as Objective, Automatable Reference Points to Test Mechanobiological Hypotheses Using Histomorphometry. J. BioMech. 2010 in review.
26. Miller RM, McBride SH, Dolejs S, Knothe UR, Knothe Tate ML. Modeling the Mechanobiology of the Periosteum to Predict & Harness its Regenerative Capacity. Proceedings of the Orthopedic Research Society Annual Meeting. 2011
27. Ng AM, Saim AB, Tan K, Tan GH, Mokhtar SA, Rose IM, Othman F, Idrus RB. Comparison of bioengineered human bone construct from four sources of osteogenic cells. J. Othop. Sci. 2005; 10:192–199.
28. Ozaki A, Tsunoda M, Kinoshita S, Saura R. Role of fracture hematoma and periosteum during fracture healing in rats: interaction of fracture hematoma and the periosteum in the initial step of the healing process. J. Orthop. Sci. 2000; 5:64–70. [PubMed: 10664441]
29. Puckett CL, Hurvitz JS, Metzler MH, Silver D. Bone formation by revascularized periosteal and bone grafts, compared with traditional bone grafts. Plast. Reconstruct. Surg. 1979; 64:361–365.
30. Rahn, B. Handbook of Biomaterials Evaluation. New York: MacMillan: 1986. “Intra Vitam Straining Techniques”; p. 471-487.
31. Rahn B. Fluorochrome labeling of bone dynamics. Europ. Cells Mat. 2003; 5:41.
32. Rehfeldt F, Engler AJ, Eckhardt A, Ahmed F, Discher DE. Cell responses to the mechanochemical microenvironment--implications for regenerative medicine and drug delivery. Adv. Drug Delivery Rev. 2007; 59:1329–1339.
33. Sakaguchi Y, Sekiya I, Yagishita K, Muneta T. Comparison of human stem cells derived from various mesenchymal tissues: superiority of synovium as a cell source. Arthritis Rheuma. 2005; 52:2521–2529.

34. Sato K, Haruyama N, Shimizu Y, Hara J, Kawamura H. Osteogenesis by gradually expanding the interface between bone surface and periosteum enhanced by bone marrow stem cell administration in rabbits. Oral Surg. Oral Med. Oral Pathol. Oral Radiol. Endod. 2010; 110:32–40. [PubMed: 20188608]
35. Sauser, B. [Accessed August 31] Technology review: faster healing for severe fractures. Tech. Rev. 2010. Available at http://www.technologyreview.com/biomedicine/24711/?a=f
36. Schmidt BL, Kung L, Jones C, Casap N. Induced osteogenesis by periosteal distraction. J. Oral maxillof. Surg. 2002; 60:1170–1175.
37. Seeman E. The periosteum--a surface for all seasons. Osteoporosis Int. 2007; 18:123–128.
38. Song MJ, Dean D, Knothe Tate ML. Situ Spatiotemporal Mapping of Flow Fields around Seeded Stem Cells at the Subcellular Length Scale. PLoS ONE. 2010; 5:e12796. [PubMed: 20862249]
39. Spitzer R, Perka C, Lindenhayn K, Zippel H. Matrix engineering for osteogenic differentiation of rabbit periosteal cells using alpha-tricalcium phosphate particles in a three-dimensional fibrin culture. J. Biomed. Mat. Res. 2002; 59:690–696.
40. Stevens MM, Marini RP, Schaefer D, Aronson J, Langer R, Shastri VP. In vivo engineering of organs: the bone bioreactor. Proc. Natl. Acad. Sci. U. S. A. 2005; 102:11450–12455. [PubMed: 16055556]
41. Taylor, J. “The periosteum and bone growth”. In: Hall, BK., editor. Bone: Bone Growth. Vol. v.6. Boca Raton, FL: CDC Press; 1992. p. 21-52.
42. Tepic S, Remiger AR, Morikawa K, Predieri M, Perren SM. Strength recovery in fractured sheep tibia treated with a plate or an internal fixator: an experimental study with a two-year follow-up. J. Orthop. Trauma. 1997; 11:14–23. [PubMed: 8990027]
43. Uddströmer L, Ritsilä V. Osteogenic capacity of periosteal grafts. A qualitative and quantitative study of membranous and tubular bone periosteum in young rabbits. Scand. J. Plast. Reconstr. Surg. 1978; 12:207–214. [PubMed: 368970]
44. Yamauchi K, Takahashi T, Funaki K, Yamashita Y. Periosteal expansion osteogenesis using highly purified beta-tricalcium phosphate blocks: a pilot study in dogs. J. Periodont. 2008; 79:999–1005. [PubMed: 18533776]
45. Yiannakopoulos CK, Kanellopoulos AD, Trovas GP, Dontas IA, Lyritis GP. Orthop. Trauma Surg. 2008; 128:117–120.
46. Zhang X, Xie C, Lin AS, Ito H, Awad H, Lieberman JR, Rubery PT, Schwarz EM, O’Keefe RJ, Guldberg RE. Periosteal progenitor cell fate in segmental cortical bone graft transplantations: implications for functional tissue engineering. J. Bone Miner. Res. 2005; 20:2124–2137. [PubMed: 16294266]
47. Zimmerman J, Knothe Tate ML. Adaptation response of live mesenchymal stem cell and nucleus shape to prescribed seeding conditions. PLoS One. 2010 In review.

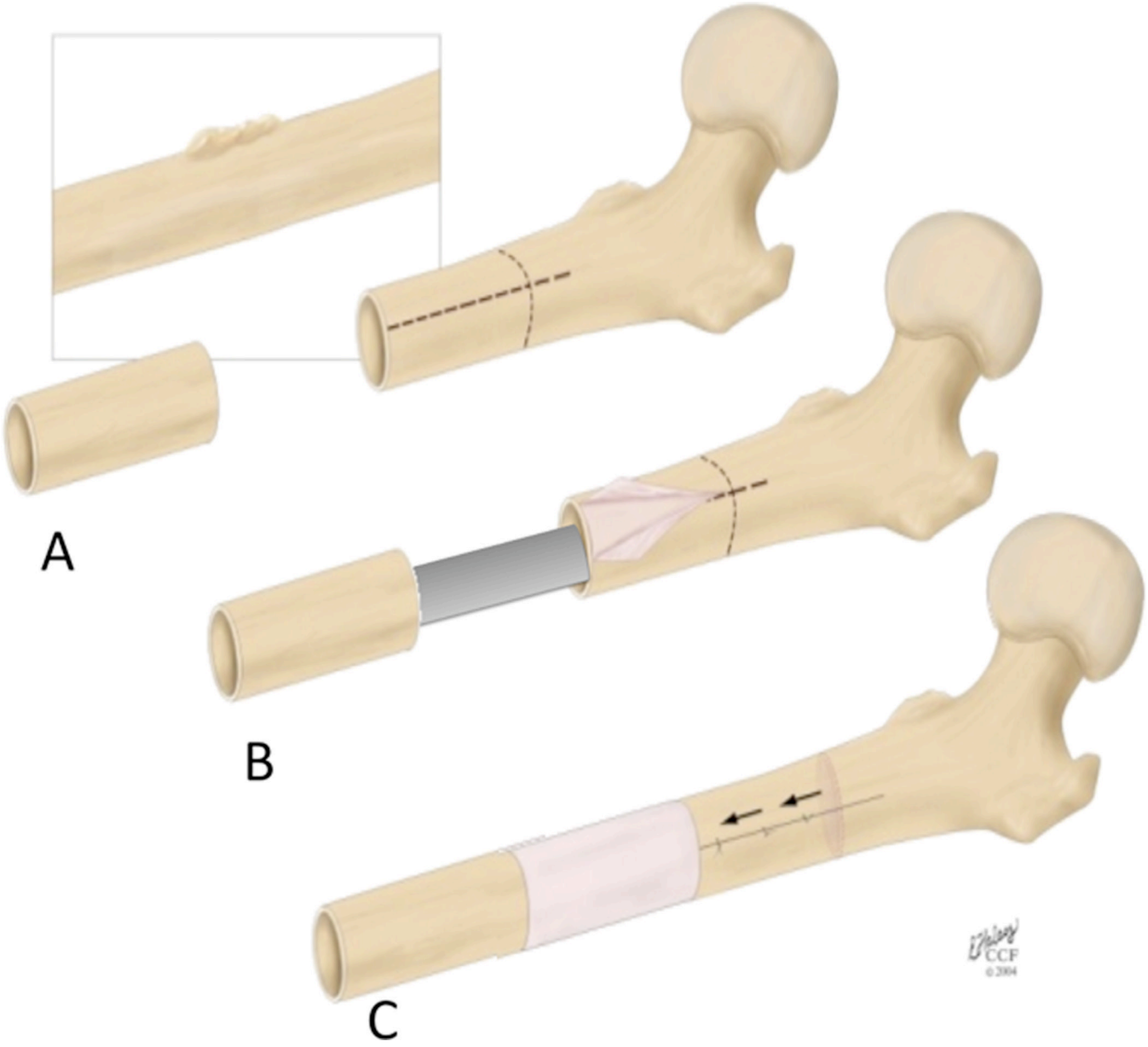

FIGURE 1. Schematic of the One-Stage Bone Transport Surgical Technique (adapted from [18])
A) A 2.54 cm sized defect is created mid-shaft B) An intramedullary nail is introduced into the reamed medullary cavity and interlocked proximally and distally to stabilize the femur. Vascularized periosteum is lifted from the bone just proximal to the large defect and an osteotomy is performed. Several 1 – 2 square mm bone chips are retained on the inner surface of the periosteum. C) The denuded bone segment is transported along the intramedullary nail and is docked in place with ligament reconstruction sutures, filling the pre-existing defect. Then the periosteum is sutured like a sleeve surrounding the "new" defect zone. Remarkably, the periosteal sleeve created by the one-stage bone transport technique fills with woven bone in as little as two weeks.[18] This technique has proven efficacious both in an ovine femoral defect model as well as in limited human cases.[18, 19, 32]

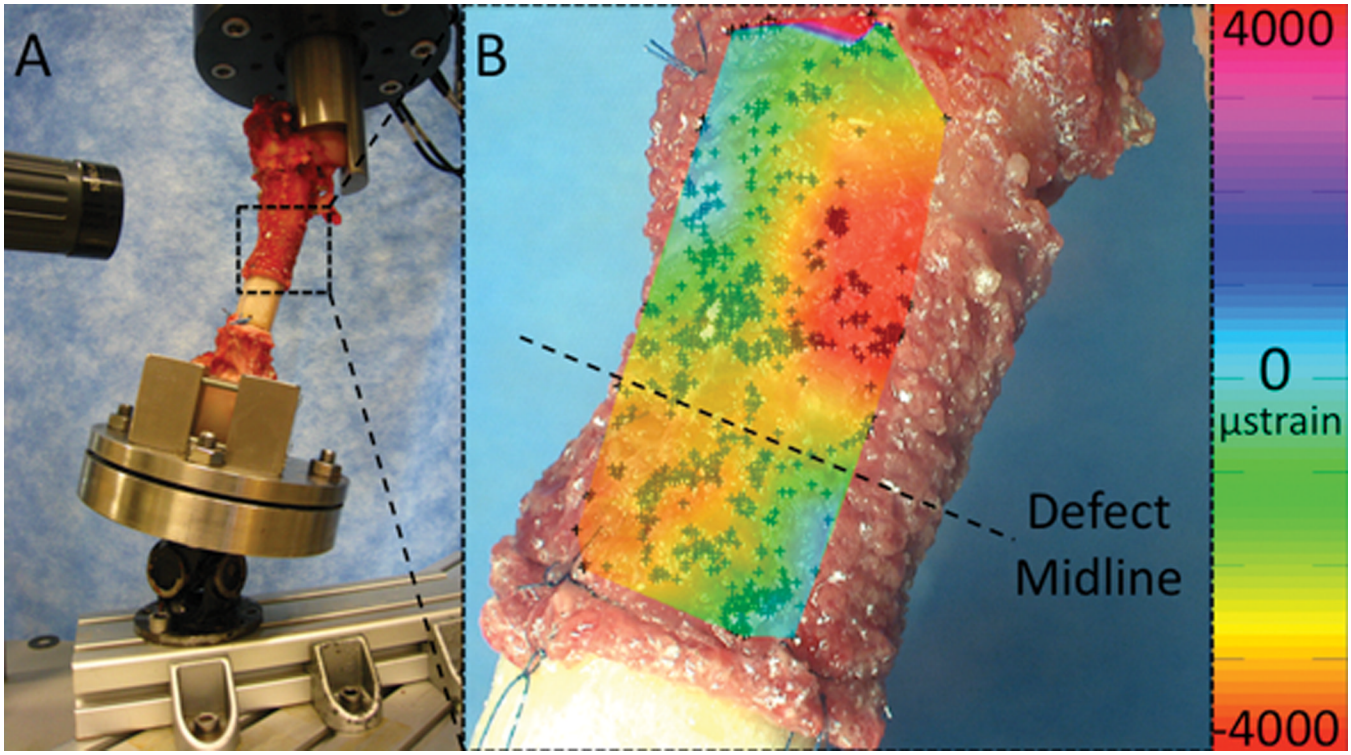

FIGURE 2.

A) Ex vivo set up for compressive loading of the femur to mimic stance shift in the first two weeks after surgery. B) Example of high definition optical strain mapping for the defect area outlined in A. The overlaid color strain map represents the actual strain at maximal load for a post-surgical femur. Dashed line defines the defect midline, the area used for correlation to histological cross-sections.

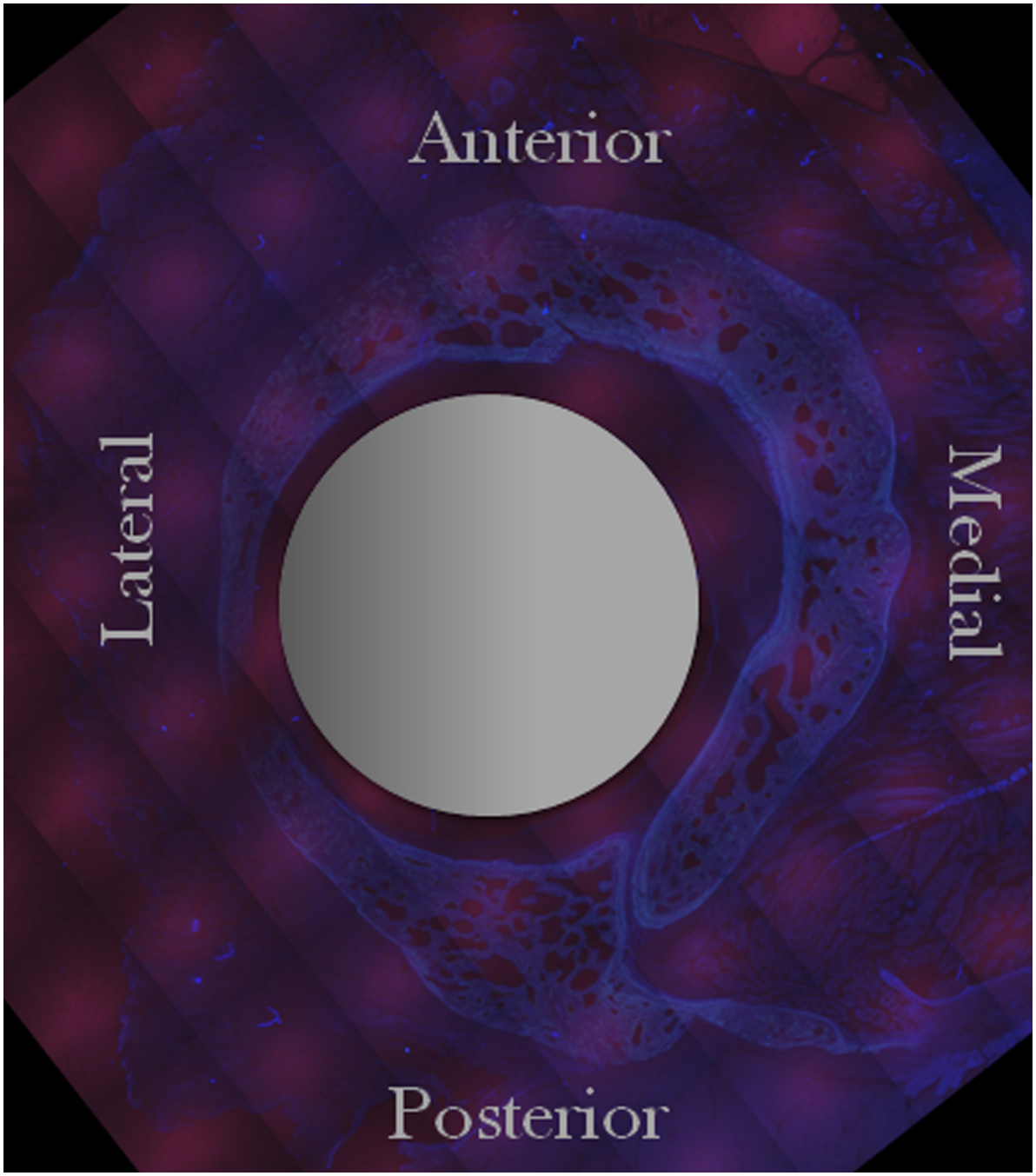

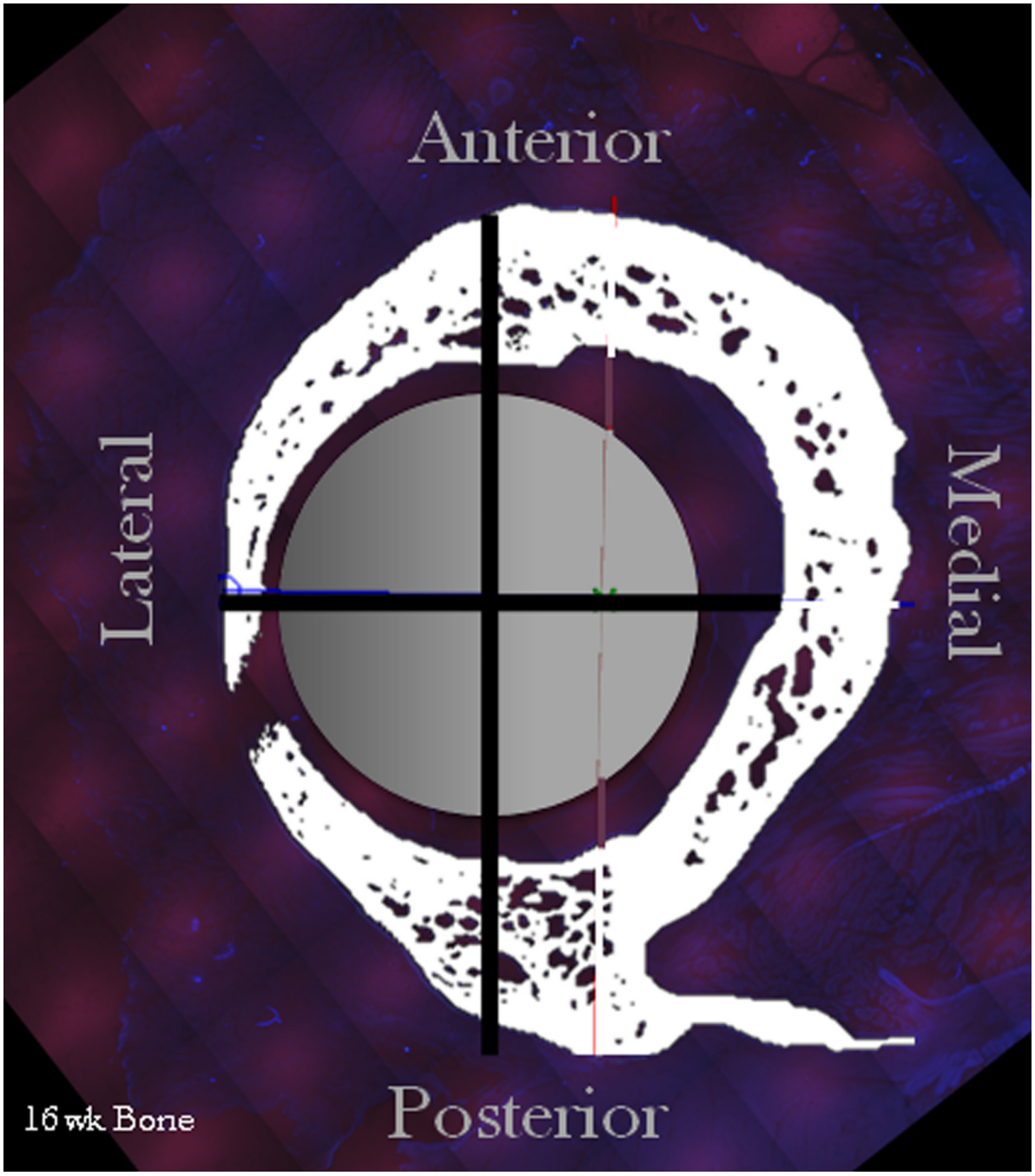

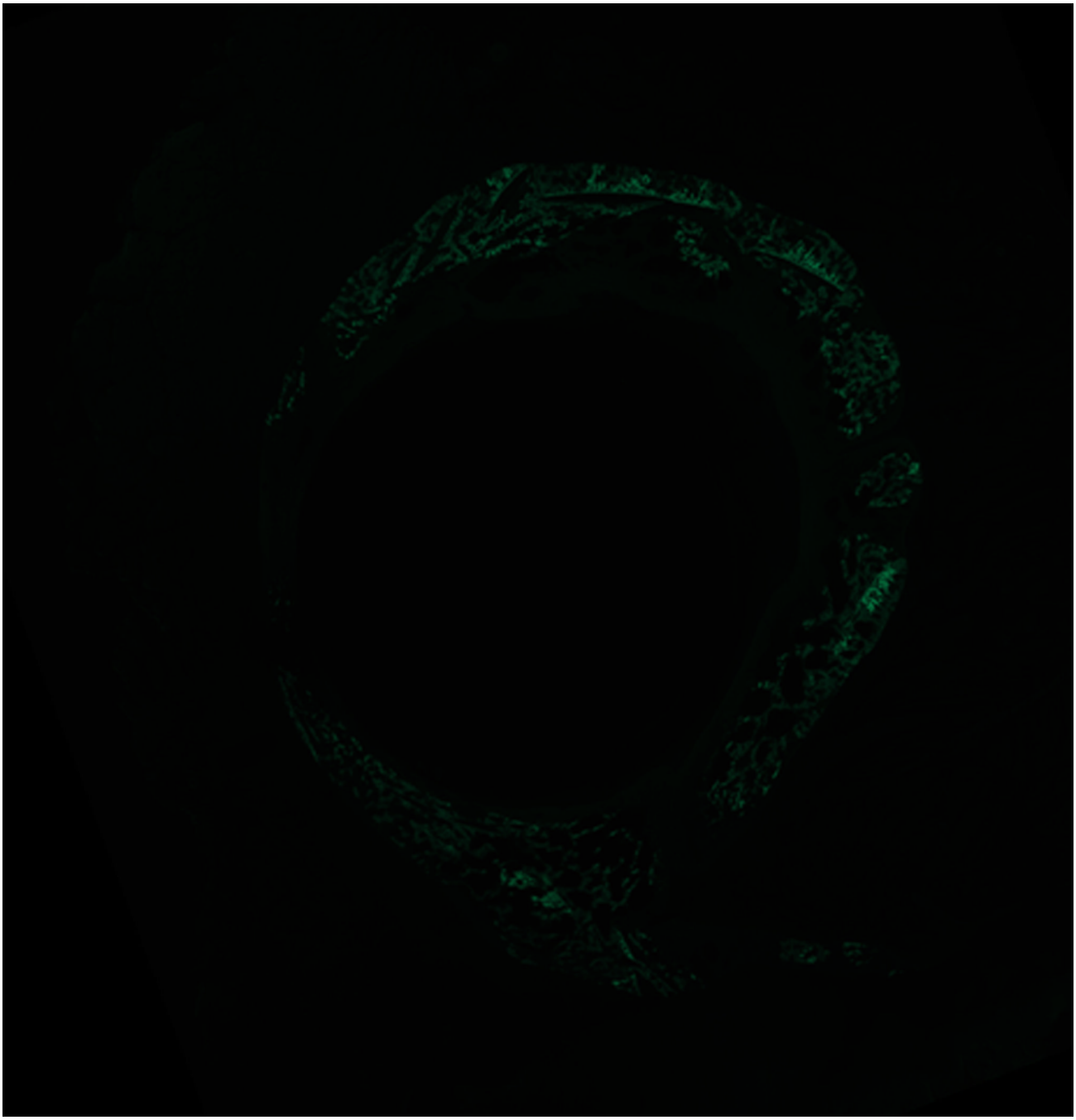

FIGURE 3.
Example of histological cross section (adapted from [44]) A) Unprocessed UV image of bone & surrounding soft tissues. B) Processed UV Image highlighting the total bone at 16 weeks (white), intermedulary rod (grey circle), and anatomical axes used as reference axes. C) Blue excitation image showing only early bone (green) that was tagged with a chelating flourochrome.

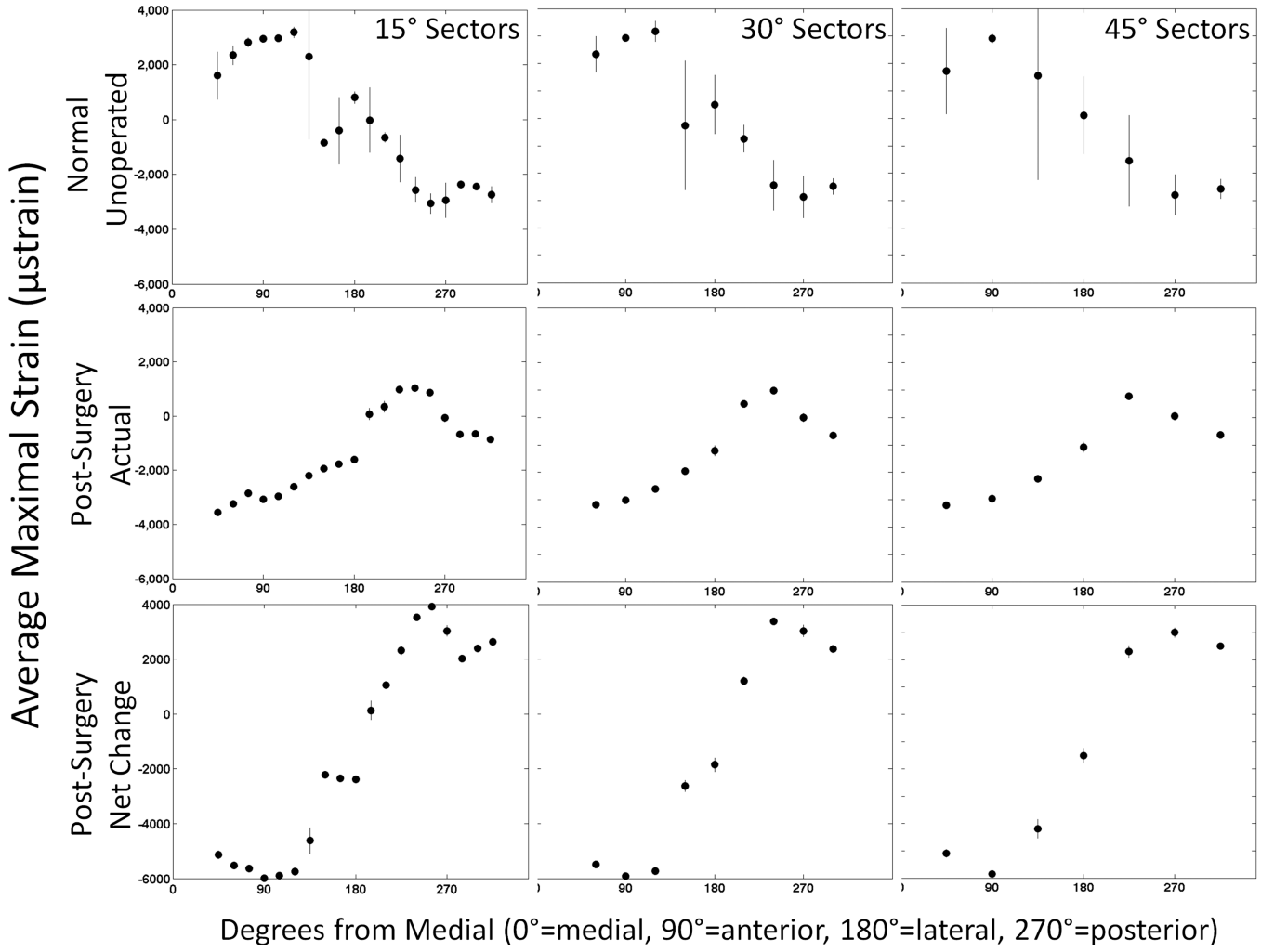

FIGURE 4.

Average maximal periosteal strains at the defect centerline per sector for normal and post-surgical femora. Strains change from anterior tensile strains and posterior compressive strains in a normal femur to anterior compressive strains and posterior tensile strains in a post-surgical femur. Error bars indicate 95% confidence intervals

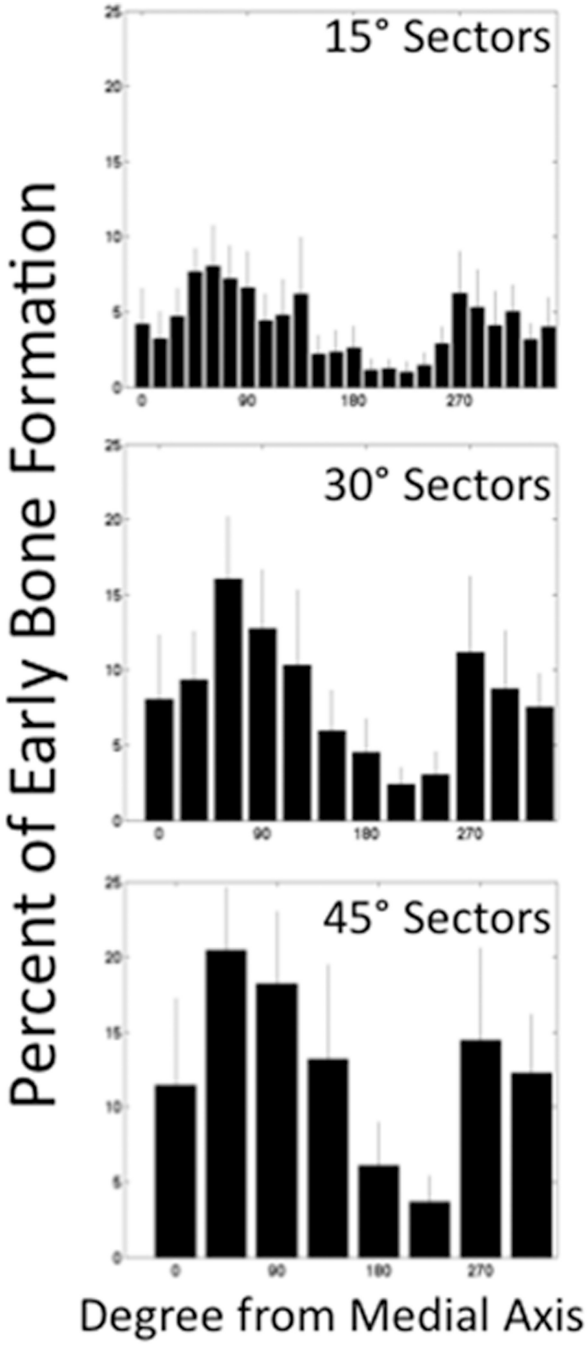

FIGURE 5.
Distribution of early bone formation. Most early bone is formed at anterior and posterior areas. Error bars indicate 95% confidence intervals

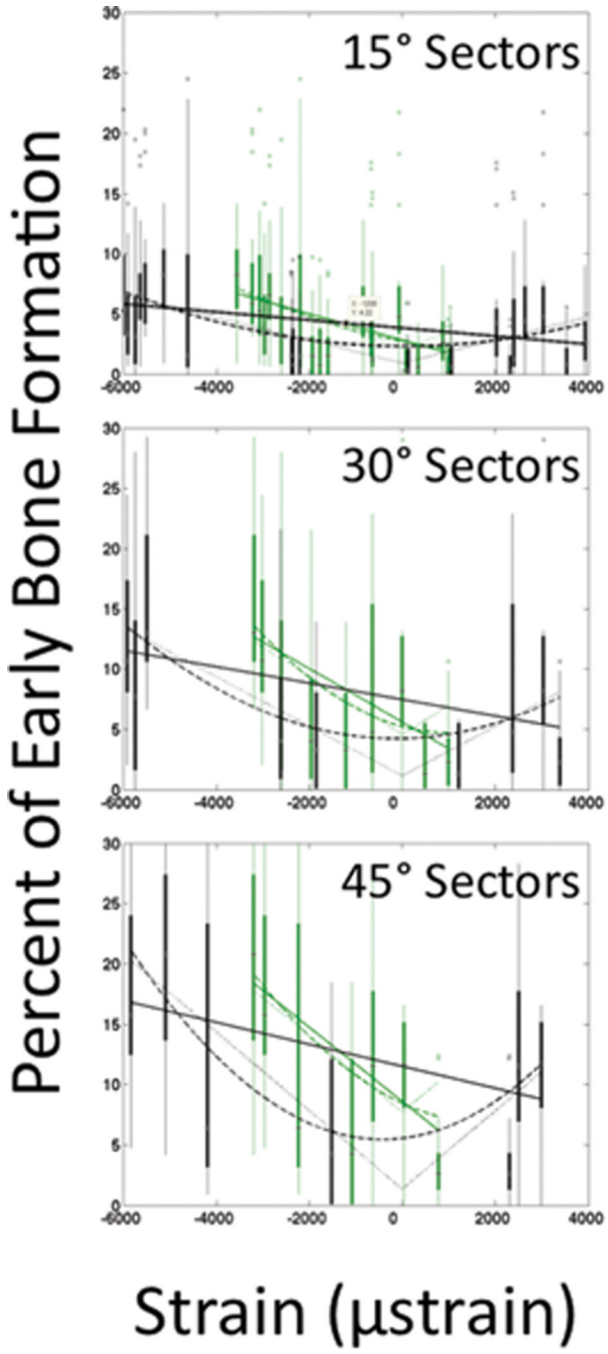

FIGURE 6.
Correlation between strain and early bone formation. There is a negative linear relationship between the actual periosteal strains and early bone formation (green data). There is a quadratic or absolute value relationship between net periosteal strains perceived by a cell and initial bone generation (black data).

Table 1

Periosteal strains at the defect midline.

Aspect	Normal Strains (με)	Actual Post-Surgical Strains (με)	Net Change (με)
Anterior	3000 to 3100	−2900 to −3500	−6000
Posterior	−2950 to −3050	650 to 1000	3900
Lateral	−800 to 800	−1800 to 100	−2400

Table 2

Fitted Models for Periosteal Strain

	˚Per Sector	**15˚**		**30˚**		**45˚**	
	Term	**Coefficient (95% CI)**	**P-Value**	**Coefficient (95% CI)**	**P-Value**	**Coefficient (95% CI)**	**P-Value**
Model 1	β_0	2.8 (2.2, 3.5)	0	5.6 (4.0, 7.2)	0	8.6 (6.1, 11.1)	0
	β_1	−1091 (−1409, −773)	0	−2208 (−3069, −1346)	0	−3062 (−4343, −1781)	0
	R^2	0.12		0.14		0.15	
Model 2	β_0	2.7 (2.1, 3.4)	0	5.2 (3.5, 7.0)	0	8.5 (6.0, 11.0)	0
	β_1	−758 (−1472, −44)	0.04	−1033 (−3070, 1004)	0.32	−1789 (−5159, 1579)	0.30
	β_2	0.13 (−0.13, 0.40)	0.04	0.50 (−0.3, 1.3)	0.32	0.49 (−0.71, 1.68)	0.30
	R^2	0.12		0.15		0.16	
Model 3	β_0	2.1 (1.3, 3.0)	0	4.6 (2.32, 6.82)	0	7.7 (4.6, 10.9)	0
	β_1	1276 (838, 1713)	0	2399 (1224, 3573)	0	3147 (1524, 4770)	0.0002
	R^2	0.09		0.09		0.11	

Table 3

Fitted Models for Net Change in Periosteal Strain

	˚Per Sector	15˚		30˚		45˚	
	Term	**Coefficient (95% CI)**	**P-Value**	**Coefficient (95% CI)**	**P-Value**	**Coefficient (95% CI)**	**P-Value**
Model 1	β_0	3.8 (3.3, 4.3)	0	7.5 (6.1, 8.8)	0	11.5 (9.5, 13.5)	0
	β_1	−334 (−468, −202)	0	−679 (−1033, −325)	0.0002	−908 (−1432, −383)	0.0008
	R^2	0.06		0.08		0.09	
Model 2	β_0	2.3 (1.4, 3.2)	0	4.2 (2.0, 6.5)	0.0003	5.6 (1.9, 9.2)	0.0032
	β_1	−9.2 (−212, 194)	0.92	74 (−472, 620)	0.79	454 (−418, 1327)	0.30
	β_2	0.13 (0.07, 0.19)	0	0.27 (0.12, 0.43)	0.0006	0.54 (0.25, 0.82)	0.0003
	R^2	0.11		0.14		0.18	
Model 3	β_0	0.93 (−0.15, 2)	0.09	1.1 (−1.8, 4.1)	0.43	1.3 (−3.2, 5.9)	0.56
	β_1	949 (674, 1224)	0	2047 (1301, 2793)	0	3242 (2042, 4443)	0
	R^2	0.11		0.15		0.19	